POWER SYSTEM SIZING AND ANALYSIS FOR ELECTRIC AIRCRAFT CONCEPTUAL DESIGN

BY

JOHN REBAND

THESIS

Submitted in partial fulfillment of the requirements
for the degree of Master of Science in Electrical and Computer Engineering
in the Graduate College of the
University of Illinois Urbana-Champaign, 2021

Urbana, Illinois

Adviser:

Professor Kiruba Sivasubramaniam Haran

ABSTRACT

This thesis presents research into and development of a suggested methodology for the sizing of an electrical power generation, distribution, and propulsion system for electric airplanes at the conceptual design level. Considerations for machine type, energy storage technology, volume packaging, and modeling are discussed.

The methodology is applied to a design study for a medium altitude, long endurance survey drone to demonstrate the process and results. Finally, future research topics in the electric aircraft design space are suggested, particularly the need for a dedicated tool for electric aircraft powertrain analysis.

To my parents, for their love, support, and patience.

ACKNOWLEDGMENTS

I must first thank my adviser, Professor Haran, for supporting my studies at UIUC. Without an electrical engineering background, I knew I would need an adviser with unusual pedagogical skill and patience to finish this degree. Professor Haran met these requirements and then some. I consider myself fortunate to have studied under him.

I also want to extend gratitude to my fellow graduate students for their kindness and the opportunity to learn from them. I was privileged to work among a group of incredibly talented and hard-working individuals. I owe much of the knowledge I gained here to Aaron Anderson, Thanatheepan Balachandran, Joshua Feldman, Jianqiao Xiao, and Max Lewis.

My colleagues at the Air Force Research Laboratory also deserve recognition for their advice and guidance through my career thus far. I look forward to continuing my work with them after graduation.

Finally, I am eternally indebted to my parents for all they sacrificed to bring me this far.

TABLE OF CONTENTS

LIST OF ABBREVIATIONS

AC	Alternating Current
BEM	Blade element momentum
BLI	Boundary Layer Ingestion
CFD	Computational Fluid Dynamics
DC	Direct Current
FEA	Fully Electric Aircraft
HEA	Hybrid-Electric Aircraft
IM	Induction Machine
MEA	More-Electric Aircraft
MTOW	Maximum Takeoff Weight
OML	Outer Mold Line
PMAD	Power Management and Distribution System
PMSM	Permanent Magnet Synchronous Machine
TOS	Time On Station
WFSM	Wound-Field Synchronous Machine

LIST OF SYMBOLS

A	Electrical Loading
AR	Wing Aspect Ratio
AR_h	Horizontal Tail Aspect Ratio
AR_v	Vertical Tail Aspect Ratio
B	Magnetic Loading
B_{ag}	Peak Airgap Magnetic Flux Density
B_h	Horizontal Tail Span
B_w	Main Wing Span
$C_{D,TO}$	Vehicle Drag Coefficient, Takeoff Conditions
$C_{D,min}$	Minimum Vehicle Drag Coefficient
$C_{L,TO}$	Vehicle Lift Coefficient, Takeoff Conditions
$C_{L,max}$	Maximum Vehicle Lift Coefficient
D_{ag}	Motor Airgap Diameter
D_{fuse}	Fuselage Depth
e	Oswald Efficiency Factor
F	Electromagnetic Force on Rotor Surface
F_w	Fuselage Width at Tail Intersection
g	Gravitational Acceleration
h	Geopotential Altitude
h_C	Cruise Altitude

h_{TO}	Takeoff Altitude
$\dot{h}$	Rate of Climb/Descent
H_e	Electrical System Energy Fraction
H_e	Electrical System Power Fraction
H_{HED}	Energy Storage High Energy Density Split
H_{HPD}	Energy Storage High Power Density Split
H_t/H_v	T-Tail Correction
I_a	Armature Current
k_w	Winding Factor
k	Lift-Induced Drag Correction
K_e	Motor Back EMF Constant
K_i	Empirical Vehicle Weight Estimation Parameters
K_{LG}	Fuselage-Mounted Gear Correction
K_t	Motor Torque Constant
K_y	Pitching Radius of Gyration
K_z	Yawing Radius of Gyration
L	Motor Active Length
L_{fuse}	Fuselage Length
L_m	Main Gear Height
L_n	Nose Gear Height
L_t	Tail Length
m	No. of Electrical Phases
m_P	Payload Mass
$m_{ES,ER}$	Energy Storage Mass to Meet Energy Requirements
$m_{ES,PR}$	Energy Storage Mass to Meet Power Requirements
N_f	No. of Control Actuator Functions
N_l	Ultimate Landing load factor

N_{mss}	No. of Main Gear Struts
N_{mw}	No. of Main Gear Wheels
N_{nw}	No. of Nose Gear Wheels
N_{ph}	No. of Phase Conductors
N_z	Ultimate Load Factor
P	No. of Rotor Pole Pairs
P_H	Hotel Load
P_{max}	Maximum Power Per Motor
P_{req}	Power Required Per Motor
P_T	Total Power
q	Dynamic Pressure
Q	Torque
S_{csw}	Control Surface Area
S_e	Elevator Area
S_f	Fuselage Wetted Area
S_G	Takeoff Run Distance
S_{ht}	Horizontal Tail Area
S_{vt}	Vertical Tail Area
S_w	Wing Area
t	Mission Segment Duration
T	Thrust
T/W	Thrust Loading
t/c	Thickness to Chord Ratio
u	Vehicle Airspeed
u_{climb}	Climb Airspeed
u_{cruise}	Cruise Airspeed
u_{stall}	Stall Airspeed

u_{TO}	Takeoff Airspeed
$U_{battery}$	Battery Energy Density
U_{fuel}	Fuel Energy Density
$W_{avionics}$	Avionics Weight, Installed
W_{dg}	Design Gross Weight
W_e	Aircraft Empty Weight
W_f	Fuel Weight
W_{fuse}	Fuselage Weight
W_{HT}	Horizontal Tail Weight
W_l	Landing Weight
W_{MG}	Main Gear Weight
W_{NG}	Nose Gear Weight
W_P	Payload Weight
W_{uav}	Avionics Weight, Uninstalled
W_{VT}	Vertical Tail Weight
W_{wing}	Wing Weight
W/S	Wing Loading
W_0	Gross Takeoff Weight
μ_g	Runway Coefficient of Friction
ρ	Air Density
σ	Rotor Shear Stress
ϕ_1	Magnetic Flux Through One Pole

CHAPTER 1

INTRODUCTION

The traditional aircraft design process has three phases: conceptual, preliminary, and detailed design. During the conceptual design phase, engineers select the vehicle configuration, perform basic performance analysis, and estimate the mass, volume, and sometimes cost of the subsystems. The inherent challenge of this initial phase is evaluating the fitness of the vehicle to the design mission at reasonable fidelity to ensure its general airworthiness, but quickly and efficiently enough to widely explore the design space before proceeding to the preliminary design phase. Conceptual design methods for "conventional" aircraft are well established. In this context, the most important feature that defines a conventional aircraft is that propulsion and power are provided by fuel-burning turbomachinery, though canonical design techniques can largely be traced back to the piston-engine era. These propulsors are usually seen in the form of turboprops or high-bypass turbofans that generate thrust and excess bleed air or shaft power for non-propulsive onboard systems.

While electric aviation is not a new idea [1], improvements in energy storage, electric machinery, power electronics, and optimization techniques have revived interest among aviation stakeholders in more-electric aircraft (MEA), broadly defined as a class of air vehicles which shift some or all of the power loads typically met by mechanical, pneumatic, and hydraulic systems to the electrical system. The consolidation of energy management from four domains to one simplifies the design and operation of the vehicle. The term hybrid-electric aircraft (HEA) describes a subset of MEA that supply some of the propulsive power electrically. The extreme case, the fully electric aircraft (FEA), derives all power for propulsive and non-propulsive systems from an electrical source. Motivation for developing practical fully electric aircraft comes from expected benefits in the context of environmental impact, dispatch reliability, propulsion integration, and cost.

Environmental Impact

A fully electric vehicle does not produce tailpipe emissions. For an aircraft, this is especially attractive because research suggests that cruise emissions have a relatively high impact on climate due to the mechanisms of interaction with the atmosphere at high altitude, on top of lowering air quality [2]. These impacts may be mitigated or eliminated if a critical mass of operating aircraft do not generate emissions in situ. However, the full magnitude of the lifetime vehicle emissions is dependent on the original generation method of the energy stored aboard the aircraft, and the equivalent emissions produced during manufacturing and end-of-life disposal should be compared with that of conventional aircraft.

Reliability/Uptime

The mechanical simplicity of electric motors and the complete elimination of certain subsystems (hydraulic and pneumatic actuators) may suggest that higher system reliability and therefore service availability could be achieved with electric aircraft. Current research is inconclusive on whether the power topology is inherently a strong predictor of system availability, but it is clear that reliability of power electronics must be maximized to achieve acceptable system reliability for commercial aviation [3]. Distribution of thrust by replacing large propulsors with many smaller ones is one way to potentially increase reliability beyond conventional designs, as the marginal impact of a single propulsor is minimal compared to twinjets. A meaningful assessment of the inherent reliability of electric aircraft compared to conventional designs may only be obtainable from analyzing maintenance and dispatch records of multiple unique designs after a completed service life [4].

Propulsion Integration

Large turbofan engines in wing-mounted podded nacelles effectively decouple the propulsion and aerodynamic performance of the vehicle. Though there are some practical operational reasons for podded engines, the popularity of this arrangement may be at least partially driven by the convenience for manufacturers of decoupling the design and analysis tasks for aerodynamic and propulsion systems. Some research suggests that these subsystems may be designed to interact cooperatively for a net vehicle performance improvement, and electric machines may be better suited than turbomachinery to

enable this tight aero-propulsive integration and realize aerodynamic benefits [5]. Critically, it is more feasible to operate many electric motors at small scale than turbines, as useful propulsion power can be produced at small scale and electrical energy distribution can be less complex than fuel distribution to multiple turbine engines.

Cost

Electric motors can have as few as one moving part and are inherently less mechanically complex than gas turbines. This reduces both manufacturing and maintenance costs of the propulsor itself, though the cost of the energy source and distribution hardware relative to the cost of a conventional fuel system must be considered. Furthermore, independence from volatile fuel prices may lower operating costs that can be passed on to customers, and make it easier for operators to predict the cost of operating a large fleet and be less susceptible to economic forces [6]. Some analysis has shown that electric aircraft could be competitive with conventional aircraft in total lifetime costs, though this is strongly dependent on realizing expected improvements in battery cost, energy density, longevity, and maintenance techniques [7, 8].

With these expected benefits motivating electric aircraft research, there are a number of major challenges that presently prevent these vehicles from entering service at large scale. Disregarding the economic and regulatory barriers, prior research has shown that technical challenges include achieving sufficient power and energy density in the sources, power electronics, and electric machines; managing onboard high-voltage systems and the resultant heat; and safety and maintenance for batteries [9, 10].

Technology improvements are being pursued in the relevant fields to meet these challenges. Design studies and research into design methods are crucial in informing our knowledge of the current status of electric aircraft technology. A robust design method should be able to help the designer determine the magnitude of the improvement in, for example, battery energy density that is required to close a certain design with useful range and payload. Aggregation of such results provides a target to compare the capabilities of contemporary hardware and assess the timelines for adoption. However, the interdisciplinary nature of aircraft design makes it difficult to assess the impact of any new technology in isolation, distinct from impacts arising from the interaction of the new technology with other elements of the vehicle. Ex-

amining many independent designs that leverage the technology is a good first step to understanding the potential benefits and drawbacks, as well as understanding the positive and negative trades with other subsystems. The need for mature designs to assess the technology impacts translates into a need for tools and methods to produce those designs.

The challenge of integrating a new technology into the field of aircraft design is probably not limited to electric powertrains. One great propulsion revolution has already occurred in the form of the Jet Age, and another may be ongoing as efforts to develop practical electric aircraft continue. Given the prevalence of empirical-derived models in the sizing and analysis of aircraft components, existing methods are often poorly suited to approach revolutionary designs that depart from the data used to generate such models. Furthermore, the design objectives do not always map perfectly from conventional components to new technologies; for example, electrical energy storage devices must be sized for power and energy density, whereas turbines can be sized for power and fuel selected for energy density. Thus, a need is demonstrated for robust, flexible aircraft design methods to assess the potential impact of arbitrary new technologies. It is desirable that such methods maintain a level of granularity appropriate for conceptual design; that is, methods that can capture the major trends in performance impact arising from technology integration, but are computationally inexpensive, usable by a broad audience, and do not require determination of detailed vehicle specifications to produce results.

In service of that goal, this thesis describes a proposed method for the sizing and analysis of a powertrain for an electric aircraft, and a design study conducted using this method. An attempt is made to describe the genesis of the method, to inform development of future methods and models that integrate arbitrary revolutionary technologies.

The remainder of the thesis is organized as follows. In Chapter 2, prior work on the development of aircraft design methods and efforts to tailor them for electric aircraft are discussed. In Chapter 3, a methodology for sizing and analyzing an aircraft powertrain for conceptual design is suggested. In Chapter 4, an example design study is conducted for an unmanned survey aircraft and the results presented. Finally, conclusions and discussion of future work are presented in Chapter 5.

CHAPTER 2

PRIOR WORK

2.1 Conventional Aircraft Design

The aircraft conceptual design process has, by some accounts, largely remained unchanged from the earliest production aircraft [11]. Canonized in Roskam [12], Raymer [13], and Anderson [14], the basic framework is illustrated in Fig 2.1.

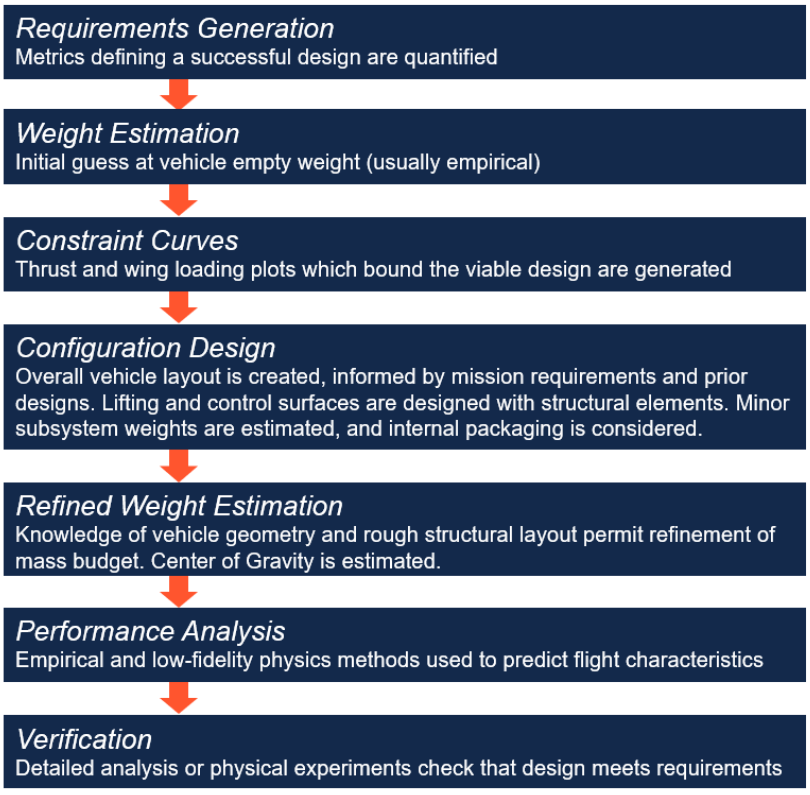

Figure 2.1: Conventional Aircraft Conceptual Design Framework

As this is an iterative, non-deterministic process; the design team may return to an earlier phase if some analysis reveals flaws in the design, or pro-

vides data to inform higher-quality results by repeating a previous analysis. In this way, the design is refined until it "closes", meaning it is predicted to meet all requirements. In some cases, no viable solution may appear and thus the mission requirements should be reconsidered in the context of the capability of the technology available. After the verification or design review is complete, the configuration, outer mold line (OML), and other important aspects of the design may be frozen so preliminary design can proceed.

Today, conceptual design is rarely, if ever, carried out by hand for any design beyond academic and hobby projects. Algorithmic methods, including genetic algorithms, gradient-based optimization, geometric programming, and analytical target cascading, have been successfully applied to "wrap" the design problem and explore the design space in much greater breadth than manual computation allows. Note that each step of the design process is an engineering discipline in and of itself. Performance, aerodynamic, propulsion, weight, and structural analysis are all included. It is important that the models and processes used in each phase to address these domains use an appropriate level of fidelity. Early in the design process, detailed, complex models are a poor choice because the turnaround time is high and not enough is known about the aircraft for those results to be meaningful. For example, if an unsteady computational fluid dynamics (CFD) solution was obtained for several flow conditions every time an OML change is made during the design study, it will be very difficult to iterate quickly and explore many designs because of the time and computational power demanded by such an analysis. The cost of complex models extends beyond the time needed to deliver results; the difficult of integration with other models or an optimizer also scales directly.

Noting this trade-off between accuracy and time to obtain results, empirical or semi-empirical models are frequently used for some if not every stage of conceptual design. These models are constructed by amalgamating data on the qualities of successful production aircraft as a function of weight or performance metrics, and permit quick calculation by hand or as part of an optimization process. Sometimes, a gain is applied to the model to account for expected technology improvements by the projected manufacturing date of the aircraft. The empirical data is often found to form a meaningful trendline, and can be used to predict the qualities of the aircraft from the mission requirements and the type of vehicle being designed. For

example, Raymer [13] presents the following equation to predict the empty weight fraction of an aircraft:

$$\frac{W_e}{W_0} = K_1 {W_0}^{K_2} K_3 \tag{2.1}$$

where K_1 and K_2 are constants linked to the class of vehicle under study, shown in Table 2.1, and K_3 is a parameter used to account for the mass of a variable sweep mechanism (equal to 1 for a fixed wing design).

Table 2.1: Empirical Dry Weight Estimation Parameters, Adapted from Raymer [13]

Vehicle Type	K_1	K_2
Glider	0.86	-0.05
General Aviation - Single Engine	2.36	-0.18
Military Fighter	2.34	-0.13
Civil Jet Transport	1.02	-0.06

The fuel weight fraction, W_f/W_0, can similarly be derived from historical data on the average fuel burn per mission segment for different propulsion architectures. Combined with the payload weight, which should be included in the mission requirements, the gross takeoff weight of the vehicle can determined by:

$$W_0 = \frac{W_P}{1 - \frac{W_f}{W_0} - \frac{W_e}{W_0}} \tag{2.2}$$

This is one example of an empirical model typically used for conceptual aircraft design. Similar models allow designers to size individual subsystems and components to meet mission requirements. Some semi-empirical models have complex formulations and take many design parameters from the vehicle as inputs, but the intent is always to quickly deliver a realistic estimate for some design variable without the detailed design information needed to construct a relevant physics model. Despite the simplicity of these methods, the performance capabilities and critical dimensions of the vehicle predicted during conceptual design are generally expected to be within 20% of the as-built vehicle [15]. Simply increasing the performance targets to which the aircraft is designed can provide high confidence that the design meets requirements [16].

Improvements in available computation power and optimization methods are driving a shift away from empirical methods to physics-based models. While empirically derived models are easy to use, computationally inexpensive, and can capture higher-order effects that are difficult to model, their usefulness is limited by the depth and breadth of the data used to generate them. Designers leveraging solely empirical models run the risk of extrapolating beyond the valid domain, resulting in a solution that fits the model but is not necessarily physically viable. Otherwise, interpolating from past data may lead to suboptimal solutions if new technology cannot be represented in the models. Physics based models instead attempt to predict the behavior of a physical system through simulation, depending on the design of a component and its interaction with other components and the environment. Application of physics-based models to the aircraft design is a potential solution to these problems, resulting in a more robust method that can handle unusual and novel designs [17].

When considering a revolutionary new topology such as an electric powertrain, the applicability of empirical design tools constructed using assumptions and trends derived from turbomachine-driven aircraft is dubious. This is not a condemnation of empirical methods; empirical methods may still be better-suited than physics models to fill some pieces of the design framework [15], and newly derived empirical models may be useful when designing an aircraft with a new technology. Rather, it is an acknowledgement that the suitability of traditional design processes to new types of vehicles should be investigated and not taken for granted.

2.2 Proposed Electric Aircraft Design Methods

There has been a significant body of work generated in recent years on proposed electric aircraft design methods, driven by scarcity of powertrain models of appropriate fidelity for conceptual aircraft design. Some notable contributions are discussed here, focusing on the overall design framework and modeling techniques for machines, power electronics, and sources.

In his dissertation, Pornet [18] approaches HEA powertrain sizing by proposing methods that can integrate within existing aircraft design frameworks, focusing on the narrow-body transport class. A major advantage of this ap-

proach is that it mitigates the challenges of onboarding designers to new tools and methods; it leverages and builds upon an existing frameworks. Starting with sizing method for conventional aircraft, the design variables unique to hybrid-electric topologies are identified: H_e and H_P represent the energy and power split, respectively, of the electrical system relative to the total quantities for the vehicle. H_P is chosen between the initial sizing of the aircraft and the domain modeling of the subsystems. Thus, the power loading (P_T/W_0) determined during initial sizing is translated to total and electrical power system requirements, which can then be used to size the powertrain. Motor modeling is conducted semi-empirically; the rotor and stator iron, magnets, and armature windings are ultimately sized based on the design power and relationships of the critical dimensions to the required volume active material and selected pole pairs. Mass can then be computed using assumed density for the material of each component and adding small gain to account for non-active material, such as cooling and mounting hardware. Some parameters, such as slot and coil number, are held constant. Modeling of the power management and distribution (PMAD) system, encompassing inverters and controllers, is accomplished via a simple empirical model, assuming a specific power and power density for each component as well as constant efficiency. These methods sufficiently capture the specifications of the powertrain relevant to conceptual design: the weight, volume, and efficiency of the components, and the power delivered by the subsystem to propulsion. Additionally, this approach allows designers to design for future technology by implementing predicted values for component specific power and power density at the target manufacturing date.

A preliminary design method for sizing a hybrid-electric, distributed propulsion aircraft is presented by de Vries, Brown, and Vos [19]. Other researchers have also taken this approach of skipping conceptual design for the electric powertrain altogether, suggesting that some representation of control scheme is necessary to have any confidence in the capability of the powertrain. Notably, this method is architecture agnostic and applicable to hybrid-electric, fully electric, and conventional powertrains. The sizing process begins by producing constraint curves, modified to include aero-propulsive interaction effects. This is accomplished by applying conservation of mass to an actuator disk model and determining the effective fluid speed over the wing and sectional lift coefficient for the propulsive span. Next, a simplified powertrain

model is developed for one of nine reference architectures. The powertrain model is used to decompose the propulsion constraint curves into individual constraint curves for the powertrain components, which the designer can use to size each piece. The power system is modeled with a linear system of equations with power transfer through each node as the state variables. The state space can be completely defined by relating the states with a gain of the efficiency, shaft power ratio, or supply power ratio on another state variable. This model assumes steady state operation, constant component efficiency, and negligible impact of transmission and heating losses. Furthermore, single component failure is accounted for by increasing the maximum power loading design target for the surviving components as required by the powertrain architecture. The final vehicle weight is estimated by a buildup of payload, fuselage, wing, powertrain, and fuel weight. Traditional empirical relationships are for the fuselage weight, assuming no impact on the structure from an electric powertrain integration. Wing weight estimation is decoupled from the fuselage due to expected higher wing loading of hybrid-electric designs; traditional empirical methods are still used. Finally, an iterative calculation is used to find the electric powertrain weight with an assumed specific power for each component.

Finger, Bil, and Braun [20] approach HEA sizing beginning with the classic sizing optimization problem: minimizing W_0 by changing the power loading (P/W) and wing loading (W/S). The electric power split, H_P, is introduced as a third independent variable. Constraint curves are generated for takeoff distance, rate of climb, stall speed, and cruise airspeed on a plot of power loading vs. wing loading. As usual, the area lying above all constraint curves is considered the design space for conventional aircraft. The new process involves selecting H_P, and moving the selecting design point down the power loading axis commensurate with the remaining turbine power. For a selection of H_P between zero and one, the designer is then informed which constraints are met by the remaining conventional power and the amount of power needed from the electrical system to make up the difference. Since the total powertrain weight is not adjusted by this method, iteration is required to adjust the location of the design point on the power-wing loading graph in accordance with the change in the total electrical and conventional power system weight. The entire power system mass, including electric components and turbomachinery, is found from the product of power loading and the

total weight estimate. A method for estimating each component weight is not covered in the paper, but a description is provided for how to compute the total "energy carrier" mass (meaning the batteries and engine propellant). The energy required is computed by analyzing the mission in small time steps rather that mission segments. Over each time step, the energy split H_e can be used to determine the power required from each system from the total energy required for flight during the time step. The power required from the engine is an input to the fuel required for that time step, and the electrical energy required is used similarly to determine the battery mass needed. This procedure develops an estimate for the power system mass with fuel and batteries over the entire mission. Adding this estimate to payload mass and the fuselage mass, from regression on empirical data, provides a prediction for W_0.

Additional relevant works consulted during this project are included in the References [21–26]. Major takeaways from review of the literature on electric aircraft design methods include:

- Some sizing approaches skip conceptual design of the powertrain altogether and approach the problem in a preliminary design context. This results from the perception that powertrain modeling is not well defined or useful at the low level of fidelity typical in conceptual design.

- Integration within existing aircraft design processes is possible and may be preferable to ground-up development of a new frameworks.

- Many proposed methods leverage existing empirical sizing functions. Some have modifications to account for expected differences in electric aircraft, but others are used as-is, with assertion that the accuracy is acceptable at the conceptual/preliminary design level.

- Steady state models are popular due to the computational expense of dynamic models. The controller design and startup concerns are left for preliminary design.

- Empirical models based on typical power and energy density are often used for the powertrain components; such models can provide reasonable estimates of weight, volume, and efficiency of the powertrain

needed to deliver the requisite propulsion without requiring detailed design of the components.

– Assuming constant efficiency for certain components, such as inverters, buses, and transmission lines, is often reasonable because there is little variation in efficiency for well-designed power electronics operating in steady state conditions within design limits.

2.3 Aircraft Powertrain Analysis Tools

Once the sizing and refinement of the powertrain are complete, the problem still remains of verifying the predicted capabilities of the sized powertrain before moving into preliminary design. For conventional aircraft, there are mature methods to accomplish these tasks in every domain. CFD solutions and wind tunnel testing can be used to demonstrate that the aerodynamic performance of the aircraft matches predictions from low-fidelity methods employed during design within reasonable tolerance. Engine performance is usually scaled from an existing design or informed by a separate engine development program. Often, simple finite element modeling (FEM) of the main structural elements is enough to ensure acceptable safety factor under the design loads.

Conversely, how sized aircraft powertrain designs should be verified at this stage is unclear. A physical testbed would provide the most accurate results, but building one would require determining specifications for all the power system components, and this work is beyond the scope of conceptual design. So, analytical tools should be considered. A useful survey of potential open-source candidates has previously been given by Milano and Vanfretti [27]. An attempt is made here to capture the set of tools an aircraft designer might consider for powertrain simulation. Relevant tools can roughly be categorized into general powertrain analysis software, MATLAB packages, and systems engineering tools.

2.3.1 General Powertrain Analysis Tools

A number of software packages for powertrain simulation are presently available, though aircraft design is generally not a primary use case.

- **FastSIM** is a tool provided by the National Renewable Energy Laboratory (NREL) for quick simulation of conventional, hydrogen-powered, hybrid, and all-electric powertrains. Two implementations of the method are available: an Excel spreadsheet and Python. Models are empirical, but performance curves are adjusted by the selected capabilities of the component (power output for electric motor, cycle depth and frequency for batteries, etc). Cost estimation is also included. Good agreement has been shown between simulation results and actual efficiency data on ground vehicle powertrains [28].

- **PSIM** is a commercial package from Powersim, Inc. One of the primary capabilities of PSIM is the modeling of motor drives, which is of obvious use for air vehicle simulation. Built-in models for several types of AC machines and lithium-ion batteries are included, and user-created component models are supported. PSIM offers a dedicated official support channel as well as community forums, video tutorials, and a library of example models to download [29].

- **Motor-CAD** is a software package for electromagnetic, thermal, and structural analysis of electric machines. A wide set of common motor types are included as well as a database of relevant materials. Motor-CAD only models electric machines, but it is useful for predicting the performance of a motor across the usable torque-speed domain, as well as the required line voltage and required power for sizing power electronics and energy storage [30].

2.3.2 MATLAB-based Tools

Widespread use of MATLAB makes it ideal for supporting collaborative research. While there is a scarcity of analysis tools developed specifically for aircraft powertrains, there are two notable entries tailored specifically for the task:

- **APST** (Aircraft Power Systems Toolbox) is a Simulink library that adds high-fidelity electrical and thermal component models. Its design philosophy was to enable a multi-domain, physics-based control framework to link control actions to system-level aircraft performance metrics. APST is free to download, but has not been widely implemented and no support exists outside the original publication describing its creation [31].

- **PowerFlow** is a package developed specifically to enable the simulation of hybrid aircraft power systems. Coupled thermal and hydraulic modeling capability is also included. Modeling of an existing commercial aircraft power system has already been demonstrated [32]. The development of PowerFlow was carried out at UIUC and sponsored by Rolls-Royce. The Numerical Propulsion System Simulation (NPSS) package is required to feed the engine models for hybrid/conventional configurations, but free academic licenses are available. PowerFlow is not publicly available nor under active development, and no dedicated support channel exists [33].

Other options for MATLAB include:

- **Autonomie** is an evolution of PSAT (Powertrain Systems Analysis Toolbox), which was developed by Argonne National Laboratory and the U.S. Department of energy to stimulate development of electric vehicles. The software allows simulation of hybrid and fully electric powertrains; models are built visually so the energy flow may be easily understood. Controller design and real-world drive cycle are included, and there is a large body of work using this tool for research on electric ground vehicles [34, 35].

- **Simscape Electrical** is the native power systems toolbox for Simulink, adding blocks for electrical machines, power electronics, and other grid components. Integration with other domains, such as the Simscape Mechanical package, is possible and custom domain models are supported. Simscape Electrical is an add-on product that must be purchased separately from the base program [36].

- **MatDyn** is power system stability analysis package that builds upon the capability of MATPOWER, another academic/research toolset.

MatDyn is open source and free to download, but does not appear to be under active development, as the documentation was last updated in 2010 [37, 38].

2.3.3 Systems Engineering Tools

A number of software tools for modeling general physical systems exist and may be applicable aircraft power systems. It is worth considering how specifically the application of a particular software package is targeted, as general-purpose tools may not possess capability to model components in sufficient detail or investigate certain behaviors. Note should be taken about whether the tool supports modeling/simulation of all the desired characteristics and behavior of a power distribution system. However, general tools may be desirable since the space of specifically aircraft-oriented options is very limited.

- **Modelica** is language for the standardization of component models, allowing simulation of a broad range of physical systems including electrical, mechanical, thermal, and hydraulic behavior. A modeling environment is required to work with Modelica libraries, and several commercial and open source environments, such as Dassualt **Dymola**, are available. Some environments support porting Modelica models to Simulink. Documentation and tutorials are available online; formal courses are provided by some environment developers [39]. Notably, Modelica has been used to model electrical systems for a large hybrid-aircraft concept [40].

- **ANSYS Twin Builder** is an instantiation of the "digital twin" concept, which describes digital models that represent physical systems in sufficient detail for accurate performance and wear prediction. Twin Builder contains multi-domain libraries for electrical, mechanical, hydraulic, and thermal interactions and also supports Modelica libraries. Because it is an Ansys product, tutorials and official community support infrastructure is robust [41].

2.3.4 Other Tools

Grid and industrial system analysis tools such as Powerworld, ETAP, and PSAT (Power Systems Analysis Toolbox) are not well-suited for aircraft design purposes. The design philosophy and assumptions make modeling aircraft systems and capturing behavior of interest at the vehicle level difficult. However, integrating battery models with grid analysis software could be useful for studying the supply logistics of operating large electric aircraft fleets.

CHAPTER 3

DEVELOPMENT OF A POWERTRAIN SIZING AND ANALYSIS METHODOLOGY

3.1 Developing the Sizing Methodology

Considering the traditional aircraft conceptual design process and recent contributions in electric aircraft design research, a methodology was developed for sizing the aircraft powertrain. First, it is useful to consider this task in context within the conceptual design framework. A formal design process for a fully electric vehicle including powertrain sizing and analysis is represented in Figure 3.1.

This N^2 diagram illustrates the information flow between the steps of the design process, showing the coupling between the various analysis domains and how design data flows between them. In this case, we are interested in the elements outline in orange; these are new processes related to power system design and analysis. While there have been attempts to codify methods for accomplishing these steps for electric propulsion aircraft, they lack the maturity to gain consensus among aircraft designers.

It is important to examine how these tasks interface with the rest of the design process. The primary driver of the powertrain sizing is the load cycle for the aircraft mission: the torque and speed required over time. The required values will change over the course of the mission, and are coupled to the desired performance, predicted vehicle mass and aerodynamic qualities, propeller design, and choice of number of propulsors. The first three of these can largely be determined by traditional methods. While number of propulsors is a design variable for any aircraft, special attention should be given to this factor for electric aircraft because realization of the benefits is closely tied to the suitability of electric propulsors to distributed propulsion configurations.

The highest power condition will almost invariably be at takeoff, and thus

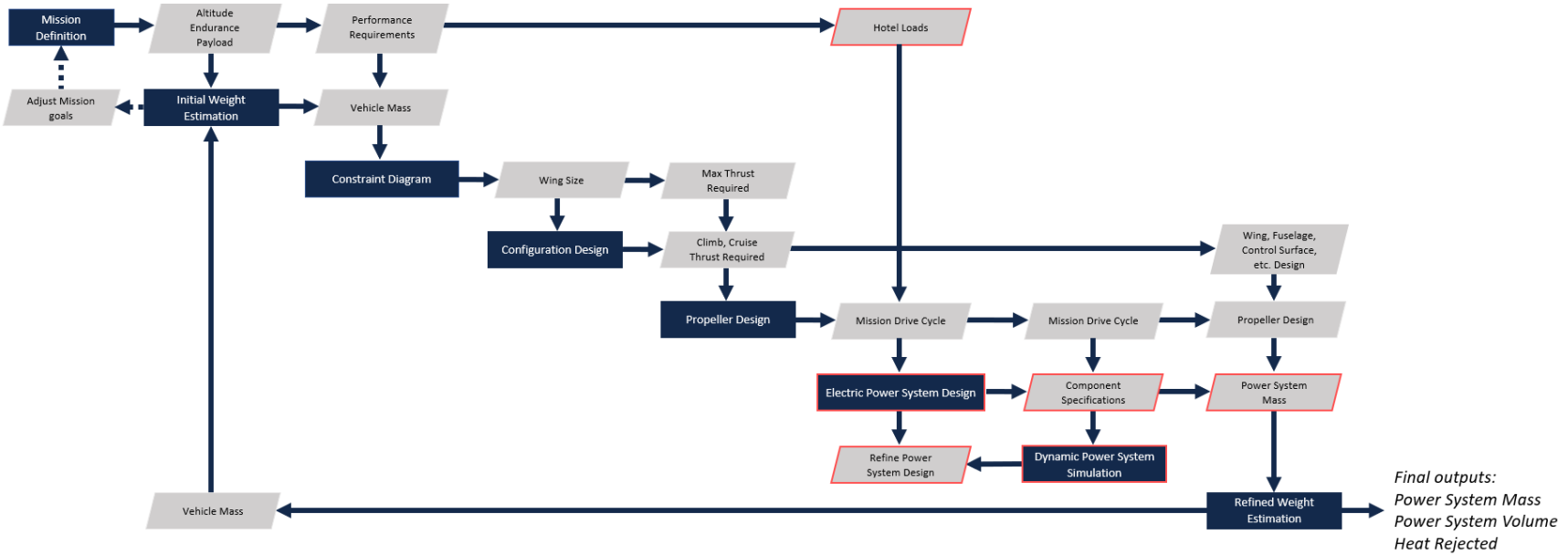

Figure 3.1: Power System Sizing N^2 Diagram for Electric Aircraft Conceptual Design

this condition may be used to size the electric motors as the amount of active material directly determines torque capability. In contrast, the time-dependent demands drive the selection of the power sources and the level of distribution of the propulsion system (i.e. number of propulsors).

When selecting the power source topology for an all-electric aircraft, most practical options for energy storage can be categorized as batteries, capacitors, or fuel cells. The primary driver in the of design an energy storage system is well illustrated by an energy density vs. power density plot for modern energy storage technology, as shown in Figure 3.2.

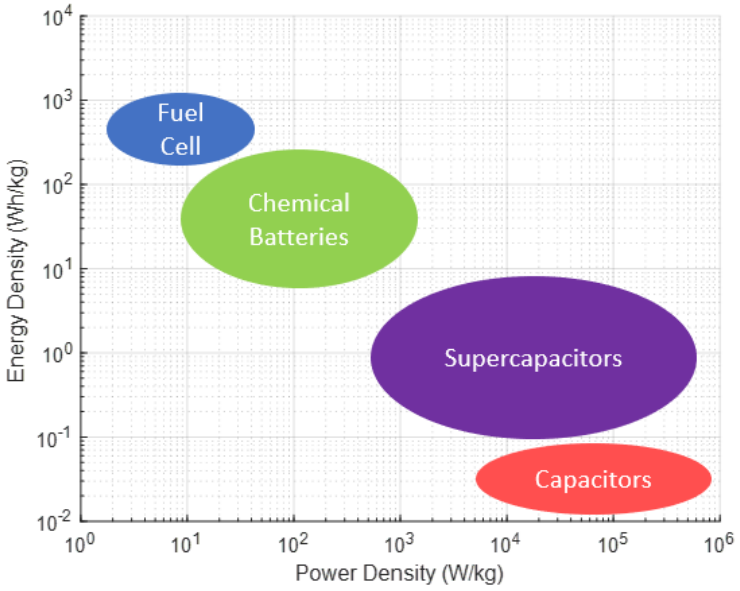

Figure 3.2: Energy Density vs. Power Density for Contemporary Energy Storage Technology (Adapted from [42])

Generally, fuel cells and chemical batteries exhibit high energy density but low power density. While these devices can store large amounts of energy, they cannot discharge this energy as quickly as super/ultracapacitors. However, the mass of capacitors required to power the aircraft over the entire mission would be much greater than a battery or fuel cell bank with the same storage capacity. Thus, a combination of high power density and high energy density storage devices provides the minimal mass solution, offering sufficient range and discharge rate at takeoff.

The ideal spanwise distribution of the propulsion system is also tied to the transient requirements, owing to the differences in the speed-efficiency

curve and scaling for propellers and motors. Additionally, the change in flight performance due to boundary layer ingestion (BLI) is tied to the percentage of span with a modified flowfield influenced by the propulsor wake, termed the propulsive span. When determining the number of propulsors on an electric aircraft, the metric of interest is the weighted overall efficiency over the entire mission. Thus, motor and propeller efficiency should be computed during every stage of the mission for each design so the relative performance of different propulsor counts can be compared.

Furthermore, it is useful to compare the mass and volume of the power system with those of a turbine engine with fuel as predicted by empirical design methods. This comparison provides context for the difficulty of integrating the electric powertrain, when the magnitude of the required change in volume and mass from conventional designs is quantified. Importantly, when a power system design has been completed, the design details can be fed back to the beginning of the process to check the weight buildup and determine if the design "closes". While typically the requirements should not be changed based on the results of any one design, determining the capabilities of aircraft leveraging a new technology may require iterating the requirements if the technology drastically impacts the capability as compared to conventional vehicles.

3.2 Powertrain Component Sizing Techniques

3.2.1 Electric Machines

For the purposes of this thesis, consideration was limited to conventional radial-flux machines. While consideration of other types of machines would be desirable for exhaustive coverage of the design space, radial flux AC machines including induction machines (IM), permanent magnet synchronous machines (PMSM), and wound-field synchronous machines (WFSM) have received the most attention as promising topologies for electric aircraft propulsion [43, 44]. A useful way of modeling the torque capability of a radial-flux machine is by analyzing shear stress on the rotor. Using this method, the following expression for torque can be developed:

$$T = \frac{\pi D_{ag}^2 L}{4} A_{peak} B_{ag,peak} \tag{3.1}$$

A derivation of this equation is provided in Appendix A. We see that torque capability can be determined if peak airgap flux density ($B_{ag,peak}$), peak electrical loading (A_{peak}), airgap diameter, and active length are known. The first two parameters can be reasonably estimated from typical values of existing machines, leaving selection of the active length and airgap diameter to determine the torque capability. Representative airgap flux density and electric loading for megawatt-class aerospace machines are 0.7 T and 21,000 A/m, respectively, at specific power of 11 kW/kg [45].

From the perspective of this model, the designer is free to select the active length and airgap diameter. While adding active material radially typically adds more torque capability than lengthening the machine, designers may select longer motor designs for aircraft design than other applications to preserve the available frontal area for the propeller. However, there are manufacturing and operational concerns that limit the practical aspect ratio of the machines. First, long rotors, especially in wound field machines, are difficult to manufacture without imbalances. At high speeds, small nonuniformities in the rotor's mass distribution can induce unsteady vibrations that decrement the machine's performance and threaten its structural integrity [46, 47]. Additionally, the stack length correlates inversely with the maximum achievable fill factor of the stator conductor [48]. Both these restrictions trade with application requirements, which may dictate the maximum allowable length of the rotor based on packaging requirements. Acknowledging these factors, an upper aspect ratio limit of eight is suggested. This should place the selected design within the realm of practical machine manufacturing, details of which can be determined during preliminary design.

While the shear stress method can be used to size the active material of the motor, it does not account for certain elements like a structural casing, bearings, and heat dissipation hardware. An auxiliary mass service factor can be applied to the motor as percentage of the active mass to account for these components. A factor of 10% of the active mass is suggested as an optimistic estimation of the auxiliary mass of electric machines designed for aircraft propulsion [49].

Though using the shear-stress perspective to size the torque capability

of electric machines offers limited accuracy, the simplicity of the method is attractive and of appropriate fidelity for conceptual aircraft design.

3.2.2 Power Electronics

As all practical onboard energy storage technologies produce direct current, inverters will likely make up the majority of total power electronics mass on the aircraft. Constant power density and specific power are commonly used to represent power electronic components in conceptual design, though the weight and volume do not actually scale linearly with power. The power density and specific power for an inverter are dependent on the device topology, operating frequency, and materials used in the construction.

The choice of an appropriate representative power density is tied to the expected service entry date of the vehicle and the designer's optimism regarding expected technology improvements. Inverters leveraging silicon carbide conductors have achieved specific power as high as 50 kW/kg in a laboratory environment, owing to high switching frequency and low thermal losses [50,51]. However, these devices are less mature than other types of inverters, and have yet to advance to the megawatt scale required in large aircraft applications.

Specific power of 19 kW/kg and power density of 14 kW/L are representative of achievable inverter specifications with contemporary, proven technologies, and are used here to size these components [44, 52, 53]. However, the trend of achievable specific power of power electronics improving by approximately one order of magnitude every 20 years has been noted by researchers and has arguably continued through the present. Thus, it is defensible for an optimistic designer to leverage this trend to predict the achievable power density of future power electronic devices [54].

3.2.3 Energy Storage

As previously discussed, a combination of high power density and high energy density energy storage technologies is more promising than a single topology. Thus, the mass ratio of one component type to the total energy storage mass should be treated as a design choice or optimization variable. H_{HED} and H_{HPD} are used to indicate the mass ratios of the high energy density

and high power density components, respectively, to the total energy storage hardware.

Similar to power electronics, the appropriate choice for the specific power and power density of the energy storage components is dependent on the device topology and optimism regarding future technology developments. Thankfully, review of recent literature is sufficient to determine expected short and long-term targets for power and energy density. Care must be taken to use the pack-level specifications, as opposed to cell-level power density often advertised by manufacturers. Typically a 20 to 30% loss in specific energy can be expected between the cell and pack level, though as little as 10% may be achievable in the near-term. Lithium-ion batteries are popular for vehicle applications, especially small air vehicles due to high energy density. As of this writing, the state of the art for lithium-ion batteries is about 200 Wh/kg specific energy at the pack level. Estimates for the required energy density of battery packs to support practical electric aviation range from 300 Wh/kg for small fixed wing vehicles up to 700 Wh/kg for large passenger aircraft and rotorcraft. Some novel battery topologies have shown promise in approaching this threshold (lithium-sulfur cells have shown cell specific energy up to 470 Wh/kg) but have yet to be demonstrated outside a laboratory environment and at scale [55].

Acknowledging the current state of the art of energy storage technologies demonstrated, the selected values to represent gravimetric and volumetric power and energy densities used for this study are shown in Table 3.1.

Table 3.1: Representative Installed Energy Storage Power and Energy Densities [56–63]

	Energy Density (Wh/L)	Specific Energy (Wh/kg)	Specific Power (kW/kg)
High energy density (Batteries/Fuel Cells)	400	200	0.4
High power density (Super/Ultracapacitors)	900	5	20

3.2.4 Transmission Hardware

The estimation of weight for transmission cables and bus bars is difficult at a conceptual level. The requirements for these components are strongly dependent on detailed design information, including the physical geometry of the distribution system, operating current (and frequency for AC), conductor materials, and insulation rating. Some aircraft configurations will have stricter requirements; wiring on variable-geometry aircraft such as tiltwings must supply power to moving components without excessive wearing or interfering with actuation [64].

In lieu of a mature empirical method, development of which necessitates data from many electric aircraft designs, a factor of 2.5% of the total mass of all other power system components is suggested to account for transmission and distribution hardware. This was derived from a detailed design study on an HEA powertrain, presented in [65].

3.3 Power System Analysis

When the sizing iteration is completed, higher-fidelity methods can be applied to verify that the design achieves required performance. The ideal aircraft powertrain analysis tool would meet all the following requirements:

- The tool should contain dynamic physics models for all the relevant powertrain components including electric machines, power electronics, busses, transmission lines, mechanical loads, and non-ideal sources (batteries, fuel cells, capacitors, and photovoltaics). These models should provide reasonably accurate predictions of performance resulting from material and geometry selections.

- The tool should be capable of simulating multiple DC and AC signals across the model, including AC signals of different frequencies.

- The tool should support automation via native API or scripting to allow integration with an optimization process and other models.

- The tool should, when adding a component to the model, default each design parameter to typical values based on some metric (power, mass,

or volume) while permitting each to be adjusted by an advanced user. This boosts usability for students and aircraft designers without limiting functionality.

- The tool should be widely available. Open source software is ideal for wide adoption, but if the software is proprietary it should at least be modestly priced and available to the general public. Software that costs many thousands of dollars per seat and requires complex licensing agreements is not conducive to collaboration.

- The tool should be officially supported, with documentation and learning resources for new users.

- The tool should be mature with known capabilities. While development of new tools is desirable, many unknowns are already present in the design process. Anchoring of previous analysis results in experimental data provides high confidence that new results are reasonable accurate.

Another useful metric for the fitness of a tool for aircraft powertrain analysis is a history of application for electric automobile powertrain analysis. The design problems are very similar, though the magnitude of and variation in power required over the mission can be much higher. Of the tools discussed in Section 2.3, Motor-CAD was selected to analyze the sized electric machines. Motor-CAD meets most of the listed requirements: it is a mature tool with demonstrated capability, offers extensive documentation and learning resources, is available at reasonable cost, and possess all the required modeling capability for electric machinery. For modeling of the entire powertrain, PSIM is suggested as the most suitable from the surveyed tools. While lacking a design philosophy specifically intended for the task, PSIM is an excellent starting point for aircraft designers interested in modeling electric powertrains.

3.4 Methodology Summary

For clarity, the proposed methodology for electric aircraft powertrain sizing is recorded here:

1. Generate top-level vehicle requirements: Payload Mass, Speed, Cruise Altitude, and Endurance/Range.
2. Conduct initial mass estimation.
3. Generate constraint curves using traditional methods. Select design point.
4. Conduct mass buildup for wing, fuselage, tail, avionics, and gear.
5. Select number of propulsors.
6. Select propeller design, or representative propeller performance model.
7. Size electric motors and power electronic hardware for maximum power condition (takeoff).
8. Select split between high power density and high energy density storage. Determine total energy storage mass to meet endurance/range and maximum power requirements.
9. Size energy transmission/distribution hardware.
10. Compile total vehicle mass buildup with sized power system.

As previously described, this is a highly iterative process, and during a study the designer may return to any earlier step to refine the design as needed.

CHAPTER 4

DESIGN STUDY

To demonstrate the use of the suggested methodology, a design study was carried out on a medium-altitude sensorcraft. Such a vehicle benefits from the high efficiency, quick turnaround time, and low noise offered by a fully electric powertrain. The design specifications for this mission are arbitrary, but set considering the capabilities of existing, conventionally-powered sensorcraft, and are given in Table 4.1

Table 4.1: Mission Requirements

Takeoff Distance (m)	S_G	300
Cruise Altitude (m)	h_c	5,000
Cruise Airspeed (kts)	u_{cruise}	200
Climb Rate (m/s)	$\dot{h}$	5
Time On Station (min)	TOS	60
Payload Mass (kg)	m_P	500
Hotel Load (kW) (Non-propulsive power)	P_H	2

4.1 Vehicle Sizing

The initial stages of vehicle sizing are briefly addressed here to obtain torque and speed requirements for the powertrain.

4.1.1 Constraint Diagram

The power/wing loading constraint curve formulations for takeoff distance, climb rate, and cruise speed given by Gudmundsson [66] are used here. The area that lies above all these curves on a plot of power loading (T/W) vs.

wing loading (W/S) represents the feasible design space, subject to the desired performance and certain vehicle assumptions. The expressions and relevant assumptions are given below.

Takeoff distance:

$$\frac{T}{W} = \frac{u_{TO}^2}{2g \cdot S_G} + \frac{q\, C_{D,TO}}{W/S} + \mu_G \left(1 - \frac{q\, C_{L,TO}}{W/S}\right) \tag{4.1}$$

where:

- u_{TO} is the required velocity for takeoff
- S_G is the length of the takeoff run
- Dynamic pressure, q, is evaluated using standard atmosphere pressure at sea level and velocity $u_{TO}/\sqrt{2}$
- μ_G is the coefficient of friction between the gear and the runway surface
- $C_{D,TO}$ is the vehicle drag coefficient in takeoff configuration and conditions
- $C_{L,TO}$ is the vehicle lift coefficient in takeoff configuration and conditions

Rate of Climb:

$$\frac{T}{W} = \frac{\dot{h}}{u_{climb}} + \frac{q}{W/S} C_{D,min} + \left(\frac{k}{q}\right)\left(\frac{W}{S}\right) \tag{4.2}$$

where:

- $\dot{h}$ is the desired climb rate
- u_{climb} is the vehicle airspeed during climb
- $C_{D,min}$ is the vehicle minimum drag coefficient, in flight
- q is evaluated using standard atmosphere pressure at climb airspeed and altitude $h_{cruise}/2$
- k is the lift-induced drag correction factor, and is given by

$$k = \frac{1}{\pi\, AR\, e} \tag{4.3}$$

where AR is the wing aspect ratio, and e is the Oswald efficiency factor, given by Raymer [13] as:

$$e = 1.78(1 - 0.045 \cdot AR^{0.68}) - 0.64 \tag{4.4}$$

Cruise Speed:

$$\frac{T}{W} = qC_{D,min}\left(\frac{1}{W/S}\right) + \left(\frac{k}{q}\right)\left(\frac{W}{S}\right) \tag{4.5}$$

where q is evaluated using standard atmosphere pressure at cruise airspeed, u_{cruise}, and altitude h_{cruise}.

Stall Speed:

$$\left(\frac{W}{S}\right)_{stall} = \frac{\rho}{2} * u_{stall}^2 * C_{L,max} \tag{4.6}$$

where:

- ρ is the air density
- u_{stall} is the stall speed
- $C_{L,max}$ is the maximum lift coefficient in cruise

Some assumptions were made regarding the qualities of the vehicle and environment to produce the constraint curves, informed by the properties of existing designs in the sensorcraft space and suggestions from popular design textbooks. These values are collected in Table 4.2.

Table 4.2: Constraint Curve Assumptions

Parameter	Assumed Value
$C_{D,min}$	0.020
$C_{D,TO}$	0.030
$C_{L,TO}$ Tail	0.85
$C_{L,max}$	1.4
AR	15
h_{TO}	0 (sea level)
u_{TO}	60 m/s
u_{stall}	30 m/s
u_{climb}	90% of u_{cruise}
μ_G	0.05

Given the performance requirements and assumptions, one can generate the constraint curve plot as displayed in Figure 4.1

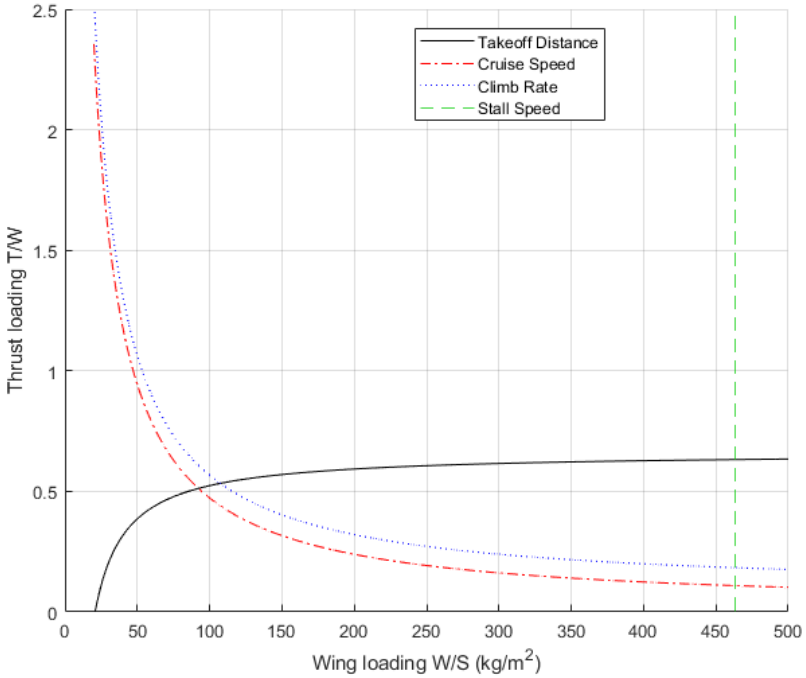

Figure 4.1: Power/Wing Loading Constraint Curve Diagram

From this constraint diagram, the minimum optimal wing loading point is approximately W/S = 105 kg/m^2 and T/W = 0.56. However, as will be demonstrated, higher wing loading will be needed to constrain the wing to a reasonable size. Therefore the maximum wing loading point that meets the stall speed constraint was selected as W/S = 463 kg/m^2 and T/W = 0.63.

4.1.2 Configuration Layout and Weight Estimation

The next step is closing the aircraft mass budget in the context of the selected wing and thrust loading. An initial guess for empty weight is normally easily obtained from trends of past aircraft in the same class. If an initial estimate for an electric aircraft is to be reasonably accurate, it must at least account for the fact that there is no distinction between empty weight and maximum weight (in the absence of dropped payloads) and for the relatively low energy density of electric energy storage compared to hydrocarbon fuel.

The MQ-9 Reaper is a high-altitude combat and surveillance platform in service with the U.S. Air Force, as well as NASA and foreign customers. Its mission is similar to the vehicle considered here, so it may be used as a reference vehicle. The maximum take-off weight (MTOW) will be scaled by ratios of endurance and specific energy to obtain an initial guess for mass of the new vehicle:

$$m = m_{ref} \frac{E_{req}}{E_{ref}} \frac{U_{fuel}}{U_{battery}} \tag{4.7}$$

According to publicly available data, MTOW for the MQ-9 is 4,760 kg and the maximum range is 1,850 km. Only the maximum airspeed is given at 240 kn, so 170 kn is assumed for cruise speed [67]. This corresponds to an endurance of approximately 5.8 h for the reference vehicle. Using 11.99 kWh/kg as a representative energy density for jet fuel [68], and 200 Wh/kg for the electrical energy storage in Equation 4.7, this produces an initial mass estimate of approximately 49,200 kg. Note that this is about an order of magnitude higher than the reference vehicle, closer to the MTOW of a small airliner than a typical unmanned survey vehicle, for a vehicle with much lower endurance. This demonstrates the vehicle-level impacts of the wide gap between specific energy of contemporary batteries and hydrocarbon fuels.

With an estimate of vehicle weight obtained, the wing area and thrust required can be determined. At 49,200 kg, the required wing area to maintain 463 kg/m^2 of wing loading is 106.26 m^2. Using the assumed aspect ratio of 15, this corresponds to wingspan of 39.92 m and mean chord length of 2.66 m. Were the minimal wing loading point at 105 kg/m^2 used here, a wingspan of 75 m would be required, which approaches the span of an Airbus A380.

These wing dimensions were used to lay out a representative vehicle configuration, taking inspiration from existing long-endurance platforms. The configuration is depicted in Figure 4.2.

Statistical methods for transport aircraft originally published by Raymer [13] were used to estimate the mass of the vehicle subsystems based on this initial design. The relevant formulas are listed here.

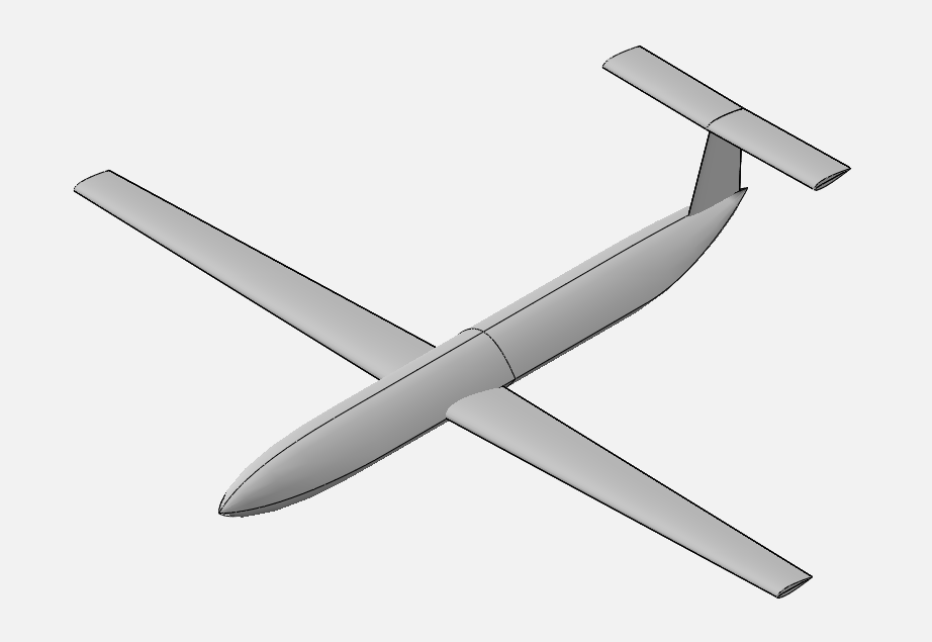

Figure 4.2: Aircraft Configuration, Version 1

- Wing:

$$W_{wing} = 0.0051\ (W_{dg}N_z)^{0.557} S_w^{0.649} AR^{0.5} (t/c)_{root}^{-0.4} (1+\lambda)^{0.1} \times (\cos\Lambda)^{-1} S_{csw}^{0.1} \tag{4.8}$$

- Fuselage:

$$W_{fuse} = 0.3280\ K_{Lg}(W_{dg}N_z)^{0.5} L_{fuse}^{0.25} S_f^{0.302} \times (1+K_{ws})^{0.04} (L_{fuse}/D_{fuse})^{0.1} \tag{4.9}$$

- Horizontal Tail:

$$W_{HT} = 0.0379\ (1+F_w/B_h)^{-0.25} W_{dg}^{0.639} N_z^{0.10} S_{ht}^{0.75} \times L_t^{-1} K_y^{0.704} (\cos\Lambda_{ht})^{-1} AR_h^{0.166} (1+S_e/S_{ht})^{0.1} \tag{4.10}$$

- Vertical Tail:

$$W_{VT} = 0.0026\ (1+H_t/H_v)^{0.225} W_{dg}^{0.556} N_z^{0.536} L_t^{-0.5} S_{vt}^{0.5} \times K_z^{0.875} (\cos\Lambda_{vt})^{-1} AR_v^{0.35} (t/c)_{root}^{-0.5} \tag{4.11}$$

- Main Gear:

$$W_{MG} = 0.0106\ W_l^{0.888} N_l^{0.25} L_m^{0.4} N_{mw}^{0.321} N_{mss}^{-0.5} u_{stall}^{0.1} \tag{4.12}$$

- Nose Gear:

$$W_{NG} = 0.032\ W_l^{0.646} N_l^{0.2} L_n^{0.5} N_{nw}^{0.45} \tag{4.13}$$

- Avionics:

$$W_{avionics} = 1.73\ W_{uav}^{0.983} \tag{4.14}$$

- Hydraulics:

$$W_{hydraulics} = 0.2673\ N_f (L_{fuse} + B_w)^{0.937} \tag{4.15}$$

Acknowledging expected weight savings by using electromechanical actuators and eliminating the hydraulic system, the control actuator weight was estimated as 50% of the hydraulics weight predicted by Equation 4.15 [69].The values used to evaluate the weight estimates are listed in Table 4.3.

Table 4.3: Weight Buildup Quantities

Variable	Name	Value	Source
AR	Main Wing Aspect Ratio	12	Design Geometry
AR_h	Horz Tail Aspect Ratio	5.71	Design Geometry
AR_v	Vert Tail Aspect Ratio	1.67	Design Geometry
B_h	Horz Tail Span	12 m	Design Geometry
B_w	Main Wing Span	39.92 m	Design Geometry
D_{fuse}	Fuselage Depth	2.8	Design Geometry
F_w	Fuselage Width at Tail Intersection	0	Design Geometry
H_t/H_v	T-Tail Correction	1	Raymer [13]
K_{LG}	Fuselage-Mounted Gear Correction	1.12	Raymer [13]
K_{ws}	-	0.2012	Raymer [13]
K_y	Pitching Radius of Gyration	4.947	Raymer [13]
K_z	Yawing Radius of Gyration	16.49 m	Raymer [13]
L_{fuse}	Fuselage Length	30	Design Geometry
L_m	Main Gear Height	1.5	Design Assumption
L_n	Nose Gear Height	1.5	Design Assumption
L_t	Tail Length	16.49 m	Design Geometry
N_f	No. of Control Actuator Functions	5	Raymer [13]
N_l	Ultimate Landing load factor	3	Raymer [13]
N_{mss}	No. of Main Gear Struts	2	Design Assumption
N_{mw}	No. of Main Gear Wheels	4	Design Assumption
N_{nw}	No. of Nose Gear Wheels	2	Design Assumption
N_z	Ultimate Load Factor	3.75	Raymer [13]
S_{csw}	Control Surface Area	$0.05*S_w$	Design Assumption
S_e	Elevator Area	$0.2*S_{ht}$	Design Assumption
S_f	Fuselage Wetted Area	246.77 m^2	Design Geometry
S_{ht}	Horz Tail Area	25.2 m^2	Design Geometry
S_{vt}	Vert Tail Area	9.6 m^2	Design Geometry
S_w	Wing Area	106.26 m^2	Design Geometry
$(t/c)_{root}$ (Main Wing)	Root Thickness/Chord Ratio	0.18	Design Assumption
$(t/c)_{root}$ (Vert Tail)	Root Thickness/Chord Ratio	0.18	Design Assumption
W_{dg}	Design Gross Weight	49,200 kg	MTOW Estimate
W_l	Landing Weight	49,200 kg	MTOW Estimate
W_{uav}	Avionics weight (uninstalled)	400 kg	Raymer [13]
λ	Wing Taper ratio	0.6	Design Geometry
Λ	Sweep at 25% MAC	1°	Design Geometry
Λ_{ht}	Horz Tail Sweep	1°	Design Geometry
Λ_{vt}	Vert Tail Sweep	15°	Design Geometry

Since this all-electric aircraft does not burn fuel, W_l is equal to the design gross weight W_{dg}. The mass estimates for each weight group are shown in Table 4.4.

Table 4.4: Vehicle Mass Estimate

Group	Mass(kg)
Wing	3,595
Fuselage	4,594
Horizontal Tail	387
Vertical Tail	181
Main Gear	385
Nose Gear	54
Avionics	617
Control Actuators	49
Payload	500
Total	10,362
Vehicle Mass Estimate	49,200
Remaining (Propulsion & Energy Storage Budget)	38,838

4.1.3 Propeller Selection

At a vehicle mass of 49,200 kg and thrust loading point of 0.63, a total of 304 kN of thrust needs to be delivered during takeoff at sea level. Assuming 16 propulsors (a relatively high number, to take advantage of distributed propulsion), this corresponds to demand of 19.1 kN on each propeller. A drag buildup was also conducted to determine the drag force and consequently thrust required in cruise, via the theory described in [70]. Total vehicle drag of 28.5 kN was estimated in cruise conditions, corresponding to 1.78 kN per propulsor.

Blade element momentum (BEM) theory was used to size a propeller capable of delivering the required thrust (assuming constant chord and pitch along the blades) and the torque and speed required to drive this propeller, assuming the tip speed is limited to 0.9 Mach [71]. While not representative of a practical propeller, this method captured the torque and speed requirements for the propulsive motors at reasonable fidelity for conceptual design. The selected propeller has 4 blades, blade chord length of 23.5 cm, blade

thickness-to-chord ratio of 0.18, and an outer diameter of 1.8 m. A plot of thrust produced and torque required for this propeller vs. airspeed at sea level conditions appears in Figure 4.3.

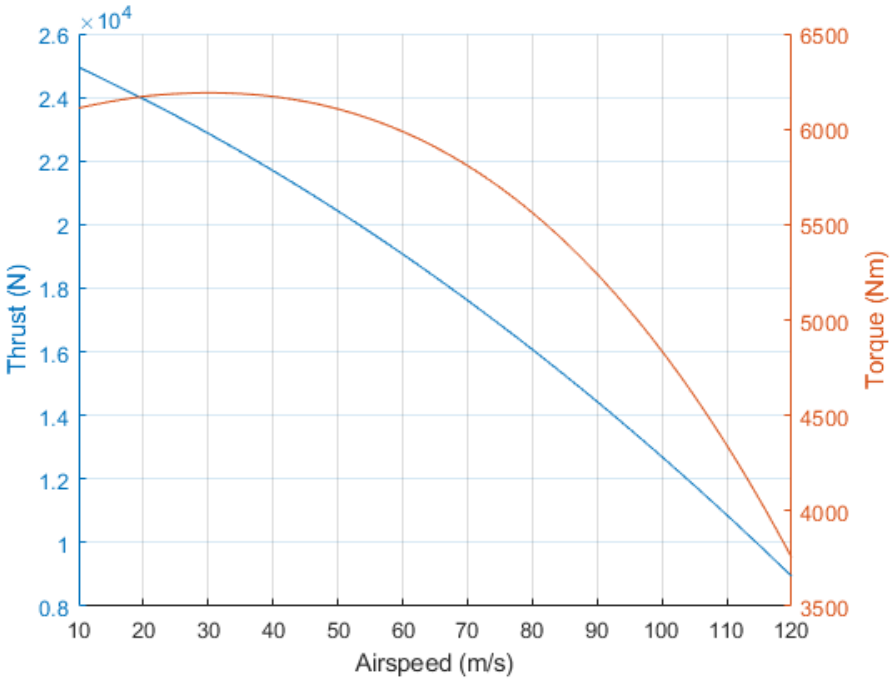

Figure 4.3: Thrust and Torque vs. Airspeed for Selected Propeller (Sea Level Conditions)

Applying the desired climb rate of 5 m/s and assuming an equal descent rate, the requisite thrust for the vehicle during each mission segment was determined, assuming aerodynamic properties halfway through climb/descent are constant through the entire mission segment [72]. The powertrain requirements, which were ultimately derived from the mission requirements and vehicle and propeller aerodynamic properties, are collected in Table 4.5.

Table 4.5: Per-Motor Mission Requirements

Segment	T (kN)	Q (N m)	Prop RPM	P_{req} (MW)	Airspeed (m/s)	Duration (min)
Takeoff	19.1	5987	3240	2.028	60	2
Climb	3.41	1477	2395	0.370	92	16.67
Cruise	1.78	831	2425	0.211	103	60
Descent	0.314	210.3	2122	0.0467	103	16.67

4.2 Powertrain Sizing

With the powertrain torque-speed requirements obtained, the individual components can be sized. First, the propulsion motors are sized for the maximum torque, 5,987 N·m, using the shear stress torque theory described in Section 3.2.1, and an assumed machine aspect ratio of two. Each motor is assumed to have a dedicated inverter so that each may be individually controlled. Again, the inverters are sized for the maximum power condition. PMAD hardware is simply sized as 2.5% of the total electrical system mass.

The energy storage mass is a function of the split ratio between high energy density and high power density devices. Starting with a chosen value of the high energy density split, H_{HED}, the average specific power and energy can be determined:

$$SP_{ave} = H_{HED} \cdot SP_{HED} + (1 - H_{HED}) \cdot SP_{HPD} \tag{4.16}$$

$$SE_{ave} = H_{HED} \cdot SE_{HED} + (1 - H_{HED}) \cdot SE_{HPD} \tag{4.17}$$

These averages can then be used to produce a mass estimate for the energy storage. Two mass estimates are conducted, one for power and one for energy:

$$m_{ES,PR} = \frac{P_{max} + P_H}{SP_{ave}} \tag{4.18}$$

$$m_{ES,ER} = \frac{1}{SE_{ave}} \sum P_{req} \cdot t \tag{4.19}$$

The summation in Equation 4.19 is computed for each mission segment. The greater of these two estimates is taken as the energy storage mass. The breakdown of the total energy storage to each type of storage device is easily recovered using the split ratios.

Finally, the propeller mass must be estimated to complete the overall propulsion system mass estimation. The adjusted Torenbeek regression method presented in [71] was used here to estimate the propeller mass, resulting in a mass of 112.29 kg. Since the mass is evaluated for each leg of the drivetrain,

the total powertrain mass is obtained by multiplying the mass of each leg by the number of propulsors:

$$m_{PT} = N_{prop} \cdot (m_{HED} + m_{HPD} + m_{PE} + m_{EM} + m_{prop}) + m_{PMAD} \quad (4.20)$$

Using the methods described previously, the vehicle mass was computed for H_{HED} between zero and one. The energy storage was sized for both energy and power requirements, with the greater of the two estimates taken at each point. The variation in system mass and volume is plotted in Figure 4.4. The total propulsion system mass buildup at the H_{HED} split for minimum mass, using contemporary technology specifications, is given in Table 4.6.

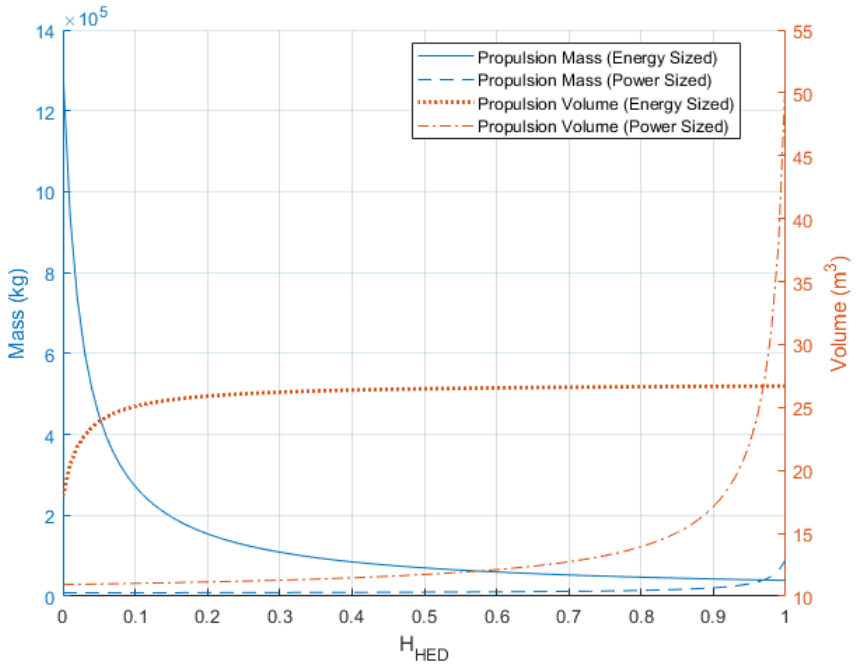

Figure 4.4: Power System Mass and Volume vs. H_{HED}

The minimum mass is 40,646 kg, at a split point of $H_{HED} = 0.97$. This result is explained by the short duration of the maximum power condition. The power demand decreases drastically after takeoff, so only a small amount of low energy density capacitors are needed. The refined mass estimate exceeds the propulsion system mass budget by only 4.65%, and the design may be closed with further iteration.

Table 4.6: Sized Propulsion System Mass Breakdown

Component	Mass (kg)	Volume (m^3)
Motors	3245	8.608
Inverters	1708	2.318
Energy Storage (HED)	31515	15.76
Energy Storage (HPD)	1313	0.0073
PMAD	1068	N/A
Propellers	1797	N/A
Total	40,646	26.69

4.3 Simulation Results

Once the powertrain sizing was completed, the motor was simulated using Motor-CAD to verify that it was sized appropriately for the application. As an effort was made to leave detailed design variables out of the sizing process, several assumptions regarding the motor were made to permit simulation. The choice of these specifications was influenced by previous research on megawatt class PMSMs [45, 73]. The specifications of the sized motor are given in Table 4.7, and a cross-sectional view of the radial build appears in Figure 4.5.

Table 4.7: PMSM Specifications

Parameter	Value
Stack Length	1.27 m
Airgap Diameter	0.637 m
Outer Diameter	0.820 m
Peak Airgap Flux Density	1.16 T
Airgap Length	4 mm
Stator Slot Count	36
Tooth Width	32 mm
Slot Depth	50 mm
Turns Count	20
Slot Fill Factor	0.5
Torque Constant (K_t)	247 Nm/A
Back EMF Constant (K_e)	379 Vs/rad
Rotor Resistance (Referred to Stator Side)	18.8 Ω
d-axis Inductance	85.31 mH
q-axis Inductance	86.44 mH

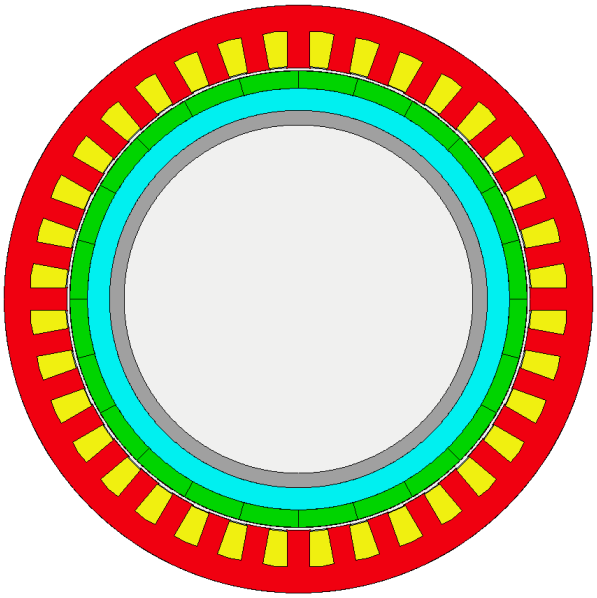

Figure 4.5: PMSM Radial Build

Note that a sinusoidal Halbach array was assumed for the rotor magnets. At the takeoff condition, the operating parameters of the motor predicted by Motor-CAD appear in Table 4.8.

Table 4.8: Motor Operating Parameters at Takeoff

Parameter	Value
DC Bus Voltage	25 kV
RMS Line Current	17.7 A
Speed	3240 RPM
Avg. Torque	6036 N·m

Thus, the Motor-CAD analysis predicts that the motor is suitable to power the aircraft.

CHAPTER 5

CONCLUSION

In conclusion, this thesis presented a methodology for conceptual design of electric aircraft and an example design study conducted using this methodology. The vehicle design actually produced by this study is highly impractical compared to vehicles of similar size, and so demonstrates the performance impact of the power and energy density of electrical propulsion systems when compared to traditional turbomachinery. The process described here can be used, at a conceptual design level, to examine the impact on vehicle performance of improvements in the volumetric and gravimetric energy and power density of powertrain components.

When considering integrating an arbitrary technology in an aircraft design process, the important consideration is how the technology interacts with existing/conventional aircraft systems. Not only do the physics change based on the domains the technology interacts with, but the design and fundamental assumptions for other subsystems may need to change to support integration. Carefully formulated design and analysis processes are needed to recognize the potential impact of exotic new technologies during conceptual aircraft design.

5.1 Future Work

The work presented here was limited to design of a fully electric topology with conventional, radial-flux AC machines, and subsequent analysis with an existing electric circuit simulation software. There are a number of obvious next steps to expand the methodology to be more robust and applicable to a wider set of vehicles.

5.1.1 Expanded Motor Topologies

While the modeling presented here is broadly applicable to the majority of machine types, there is some research that suggests axial-flux machines and more exotic topologies could be well suited as aircraft propulsors [74, 75]. Some DC machines may also be worth consideration [43].

Furthermore, superconducting machines offer extreme power density at the cost of integrating a robust cooling system, and are being seriously considered for this application [76]. The major obstacle to implementing superconducting machines in aircraft sizing is the need to account for non-active mass as a function of torque and speed capabilities. Considering superconducting machines during conceptual design will certainly require modeling of the thermal management hardware.

5.1.2 Aero-propulsive Integration

A major benefit of an electric powertrain is the ease of distributing the propulsive area across many small motors, permitting beneficial interaction with the vehicle aerodynamics. The propeller model used here did not account for the interaction with the fuselage, lifting surfaces, or nearby propellers. A more complete design study would take these effects into account, quantifying the change in required power from the propulsion system when aero-propulsive interactions are present.

5.1.3 Non-Propulsive Loads

The focus of this method was on the propulsive power, with a small hotel load included to represent avionics, communications, and payload. One important electrical load not accounted for here is the power demanded by electromechanical flight control actuators. If regenerative braking is used when returning deflected control surfaces to normal condition, the net energy demand could potentially be very small. The precise magnitude of required energy needs to be determined from detailed performance analysis on a representative vehicle with a mission that includes the highest expected number and magnitude of control deflections.

5.1.4 Purpose-built Design Tools

A major obstacle to the design of electric aircraft is the lack of purpose-built tools for analyzing aircraft power systems. Requirements for such a tool were discussed in this thesis, but the key capabilities are accurate models for all the relevant powertrain components and the ability to interface with other domain models, such as that for a propeller. In addition to powertrain analysis, low-fidelity aerodynamic analysis software for integrated aero-propulsive systems is a major capability gap that prevents fully realizing the performance potential of an optimized electric aircraft during conceptual design.

5.1.5 Cost Estimation

Economic forces will undoubtedly play a role in the speed and breadth at which electric aircraft are adopted. Development, manufacturing, operating, maintenance, and retirement costs are all relevant to understanding the cost difference between conventional and electric power in practice. Until major advancements in power and energy density of powertrain components, these comparisons need to extend beyond just the materials cost of individual airframes. Electric aircraft are not yet competitive from the vehicle-level perspective, but may excel in analysis of fleet-level economics and representative costs of environmental impact.

5.1.6 Empirical Verification

The ultimate test of an aircraft design method is whether the results can be carried through detailed design and manufacturing to produce an airworthy vehicle capable of completing the design mission. Full-scale demonstration of a statistically significant number of designs is infeasible, but incremental progress towards empirical verification of the methodology can be made by leveraging advanced analytical methods and subscale experiments.

APPENDIX A

SHEAR STRESS TORQUE DERIVATION

One method to understand the torque developed by a radial-flux machine is by examining the shear stress at the rotor surface and subsequently the torque. The shear stress is equal to the product of electrical loading and magnetic loading.

$$\sigma = AB \tag{A.1}$$

where

The electrical loading, A, is the total ampere turns (magnetomotive force) divided by the circumference of the air gap:

$$A = \frac{2mN_{ph}I_a}{\pi D_{ag}}$$

The magnetic loading, B, is the magnetic flux per rotor pole divided by the surface area of a pole:

$$B = \frac{\phi_1 2P}{\pi D_{ag} L}$$

The magnetic loading is effectively equal to the average flux density in the airgap. The force on the rotor is the product of shear stress and surface area of the rotor surface:

$$F = \sigma \pi D_{ag} L \tag{A.2}$$

The shear stress varies with ($\sin^2$) around the airgap. The average shear stress is:

$$\sigma_{avg} = \frac{A_{peak} B_{ag,peak}}{2} \tag{A.3}$$

The steady state torque on the rotor is thus:

$$\begin{aligned} T &= \sigma_{avg}\pi\frac{D_{ag}^2}{2}L \\ &= \pi\frac{A_{peak}B_{ag,peak}}{2}\frac{D_{ag}^2L}{2} \\ &= \frac{\pi}{2}\frac{D_{ag}^2L}{2}\left(\frac{2mN_{ph}I_{a,peak}}{\pi D_{ag}}\right)B_{ag,peak} \end{aligned} \tag{A.4}$$

Furthermore, the effect of distributed windings can be included and the expression written in terms of RMS current.

$$\begin{aligned} T &= k_w\frac{\pi}{2}\frac{D_{ag}^2L}{2}\left(\frac{2mN_{ph}\sqrt{2}I_{a,rms}}{\pi D_{ag}}\right)B_{ag,peak} \\ &= k_w\frac{\pi}{2}\frac{D_{ag}L}{2}\left(\frac{2mN_{ph}\sqrt{2}I_{a,rms}}{\pi}\right)B_{ag,peak} \\ &= k_w\frac{D_{ag}L}{2}\left(mN_{ph}\sqrt{2}I_{a,rms}\right)B_{ag,peak} \\ &= k_w\frac{m}{\sqrt{2}}D_{ag}LN_{ph}I_{a,rms}B_{ag,peak} \end{aligned} \tag{A.5}$$

This equation indicates that, theoretically, two machines of the same geometry, materials, and winding pattern should have the same torque capability. Further reading on the shear stress theory can be found in [77, 78].

REFERENCES

[1] L. A. Costello, "State of the art of piloted electric airplanes, NASA's centennial challenge data and fundamental design implications," M.S. thesis, Embry-Riddle Aeronautical University, Daytona Beach, FL, 2011.

[2] O. Søvde et al., "Aircraft emission mitigation by changing route altitude: A multi-model estimate of aircraft NO_x emission impact on O_3 photochemistry," *Atmospheric Environment*, vol. 95, pp. 468–479, June 2014.

[3] P. Bertorelli, "Electric aircraft reliability: Not so simple," May 2015, AVweb. [Online]. Available: https://www.avweb.com/ownership/electric-aircraft-reliability-not-so-simple/

[4] R. Jones, "The more electric aircraft: The past and the future?" in *IEEE Colloquium on Electrical Machines and Systems for the More Electric Aircraft*, 1999.

[5] A. Wick, J. Hooker, C. Hardin, and C. Zeune, "Integrated aerodynamic benefits of distributed propulsion," in *53rd AIAA Aerospace Sciences Meeting*. American Institute of Aeronautics and Astronautics, Jan. 2015. [Online]. Available: https://doi.org/10.2514/6.2015-1500

[6] "Highlights of GAO-14-331: Impact of fuel price increases on the aviation industry," United States Government Accountability Office, sep 2014. [Online]. Available: https://www.gao.gov/assets/670/666127.pdf

[7] K. Ploetner et al., "Operating cost estimation for electric powered transport aircraft," in *AIAA Aviation Technology, Integration, and Operations Conference*, 2013.

[8] A. Schäfer et al., "Technological, economic and environmental prospects of all-electric aircraft," *Nature Energy*, vol. 4, pp. 160–166, Feb 2019.

[9] I. Bolvashenkov, J. Kammermann, and H.-G. Herzog, "Electrification of helicopter: Actual feasibility and prospects," in *2017 IEEE Vehicle Power and Propulsion Conference (VPPC)*. IEEE, Dec. 2017. [Online]. Available: https://doi.org/10.1109/vppc.2017.8330883

[10] J. Kammermann, I. Bolvashenkov, K. Tran, H.-G. Herzog, and I. Frenkel, "Feasibility study for a full-electric aircraft considering weight, volume, and reliability requirements," in *2020 International Conference on Electrotechnical Complexes and Systems (ICOECS)*. IEEE, Oct. 2020. [Online]. Available: https://doi.org/10.1109/icoecs50468.2020.9278461

[11] J. D. Anderson, "Airplane design methodology: Setting the gold standard," *AIAA Journal*, vol. 44, no. 12, pp. 2817–2819, Dec. 2006. [Online]. Available: https://doi.org/10.2514/1.27756

[12] J. Roskam, *Airplane Design*. Lawrence, KS: DARcoporation, 1997, vol. Part I - Preliminary Sizing of Airplanes.

[13] D. Raymer, *Aircraft Design: A Conceptual Approach*. Washington, DC: AIAA, 1992.

[14] J. Anderson, *Aircraft Performance And Design*. Boston, MA: WCB McGraw-Hill, 1999.

[15] S. A. Brandt, M. Post, D. W. Hall, F. Gilliam, T. Jung, and T. R. Yechout, "The value of semi-empirical analysis models in aircraft design," in *16th AIAA/ISSMO Multidisciplinary Analysis and Optimization Conference*. American Institute of Aeronautics and Astronautics, June 2015. [Online]. Available: https://doi.org/10.2514/6.2015-2486

[16] D. Neufeld, "Multidisciplinary aircraft conceptual design optimization considering fidelity uncertainties," Ph.D. dissertation, Ryerson University, Toronto, ON, 2010.

[17] J. Y. Kao, T. White, M. Leonard, G. Reich, and S. Burton, "Structural sizing of aircraft wings and fuselages in conceptual multidisciplinary design processes," in *2018 Multidisciplinary Analysis and Optimization Conference*. American Institute of Aeronautics and Astronautics, June 2018. [Online]. Available: https://doi.org/10.2514/6.2018-3877

[18] C. Pornet, "Conceptual design methods for sizing and performance of hybrid-electric transport aircraft," Ph.D. dissertation, Technical University Munich, Munich, Germany, 2018.

[19] R. de Vries, M. Brown, and R. Vos, "Preliminary sizing method for hybrid-electric distributed-propulsion aircraft," *Journal of Aircraft*, vol. 56, no. 6, pp. 2172–2188, Nov. 2019. [Online]. Available: https://doi.org/10.2514/1.c035388

[20] D. F. Finger, C. Bil, and C. Braun, "Initial sizing methodology for hybrid-electric general aviation aircraft," *Journal of Aircraft*, vol. 57, no. 2, pp. 245–255, Mar. 2020. [Online]. Available: https://doi.org/10.2514/1.c035428

[21] I. Chakraborty, "Subsystem architecture sizing and analysis for aircraft conceptual design," Ph.D. dissertation, Georgia Institute of Technology, Atlanta, GA, 2015.

[22] F. Orefice, P. D. Vecchia, D. Ciliberti, and F. Nicolosi, "Aircraft conceptual design including powertrain system architecture and distributed propulsion," in *AIAA Propulsion and Energy 2019 Forum*. American Institute of Aeronautics and Astronautics, Aug. 2019. [Online]. Available: https://doi.org/10.2514/6.2019-4465

[23] F. Centracchio, M. Rossetti, and U. Iemma, "Approach to the weight estimation in the conceptual design of hybrid-electric-powered unconventional regional aircraft," *Journal of Advanced Transportation*, vol. 2018, pp. 1–15, Oct. 2018. [Online]. Available: https://doi.org/10.1155/2018/6320197

[24] J. Xiao, N. Salk, and K. Haran, "Conceptual design of an eVTOL air shuttle for rapid intercity transport," in *2020 IEEE Power and Energy Conference at Illinois (PECI)*. IEEE, Feb. 2020. [Online]. Available: https://doi.org/10.1109/peci48348.2020.9064631

[25] C. Pornet, C. Gologan, P. C. Vratny, A. Seitz, O. Schmitz, A. T. Isikveren, and M. Hornung, "Methodology for sizing and performance assessment of hybrid energy aircraft," *Journal of Aircraft*, vol. 52, no. 1, pp. 341–352, Jan. 2015. [Online]. Available: https://doi.org/10.2514/1.c032716

[26] M. Hoogreef, R. de Vries, T. Sinnige, and R. Vos, "Synthesis of aero-propulsive interaction studies applied to conceptual hybrid-electric aircraft design," in *AIAA Scitech 2020 Forum*. American Institute of Aeronautics and Astronautics, Jan. 2020. [Online]. Available: https://doi.org/10.2514/6.2020-0503

[27] F. Milano and L. Vanfretti, "State of the art and future of OSS for power systems," in *2009 IEEE Power & Energy Society General Meeting*. IEEE, July 2009. [Online]. Available: https://doi.org/10.1109/pes.2009.5275920

[28] A. Brooker, J. Gonder, L. Wang, E. Wood, S. Lopp, and L. Ramroth, "FASTSim: A model to estimate vehicle efficiency, cost and performance," in *SAE Technical Paper Series*. SAE International, Apr. 2015. [Online]. Available: https://doi.org/10.4271/2015-01-0973

[29] "PSIM," Powersim Inc., accessed 3 Aug 2020. [Online]. Available: https://powersimtech.com/products/psim/

[30] "Motor-CAD: Motor design," Motor Design Ltd., accessed 20 Aug 2020. [Online]. Available: https://www.motor-design.com/motor-cad/

[31] M. A. Williams, "A framework for the control of electro-thermal aircraft power systems," Ph.D. dissertation, University of Illinois at Urbana-Champaign, Urbana, IL, 2017.

[32] M. Williams, S. Sridharan, S. Banerjee, C. Mak, C. Pauga, P. Krein, and A. Alleyne, "Powerflow: A toolbox for modeling and simulation of aircraft systems," in *SAE AeroTech Congress & Exhibition*, 2015.

[33] C. Mak, "Modeling and simulation of commercial aircraft electrical systems," M.S. thesis, University of Illinois at Urbana-Champaign, Urbana, IL, 2015.

[34] "Success story: PSAT accurately simulates advanced vehicles," United States Department of Energy, Jan. 2004. [Online]. Available: https://www1.eere.energy.gov/vehiclesandfuels/pdfs/success/psat.pdf

[35] S. Halbach, P. Sharer, S. Pagerit, A. P. Rousseau, and C. Folkerts, "Model architecture, methods, and interfaces for efficient math-based design and simulation of automotive control systems," in *SAE Technical Paper Series*. SAE International, Apr. 2010. [Online]. Available: https://doi.org/10.4271/2010-01-0241

[36] "Simscape electrical," n.d., The MathWorks, Inc., accessed 1 Aug 2020. [Online]. Available: https://www.mathworks.com/products/simscape-electrical.html

[37] "MatDyn," n.d., The MathWorks, Inc., accessed 1 Aug 2020. [Online]. Available: https://www.mathworks.com/products/simscape-electrical.html

[38] S. Cole and R. Belmans, "MatDyn, a new MATLAB-based toolbox for power system dynamic simulation," *Transactions on Power Systems*, vol. 26, no. 3, 2011.

[39] "Modelica language," Modelica Association, accessed 1 Aug 2020. [Online]. Available: https://www.modelica.org/modelicalanguage

[40] M. Podlaski, L. Vanfretti, H. Nademi, P. J. Ansell, K. S. Haran, and T. Balachandran, "Initial steps in modeling of CHEETA hybrid propulsion aircraft vehicle power systems using Modelica," in *AIAA Propulsion and Energy 2020 Forum*. American Institute of Aeronautics and Astronautics, Aug. 2020. [Online]. Available: https://doi.org/10.2514/6.2020-3580

[41] "Ansys twin builder capabilities," Ansys, Inc., accessed 1 Aug 2020. [Online]. Available: https://www.ansys.com/products/systems/ansys-twin-builder/twin-builder-capabilities

[42] Y. Zhang, J. Jiang, Y. An, L. Wu, H. Dou, J. Zhang, Y. Zhang, S. Wu, M. Dong, X. Zhang, and Z. Guo, "Sodium-ion capacitors: Materials, mechanism, and challenges," *ChemSusChem*, vol. 13, no. 10, pp. 2522–2539, Mar. 2020. [Online]. Available: https://doi.org/10.1002/cssc.201903440

[43] A. D. Anderson, N. J. Renner, Y. Wang, D. Lee, S. Agrawal, S. Sirimanna, K. Haran, A. Banerjee, M. J. Starr, and J. L. Felder, "System weight comparison of electric machine topologies for electric aircraft propulsion," in *2018 AIAA/IEEE Electric Aircraft Technologies Symposium*. American Institute of Aeronautics and Astronautics, July 2018. [Online]. Available: https://doi.org/10.2514/6.2018-4983

[44] R. Jansen, C. Bowman, A. Jankovsky, R. Dyson, and J. Felder, "Overview of NASA electrified aircraft propulsion (EAP) research for large subsonic transports," in *53rd AIAA/SAE/ASEE Joint Propulsion Conference*. American Institute of Aeronautics and Astronautics, July 2017. [Online]. Available: https://doi.org/10.2514/6.2017-4701

[45] A. Yoon, J. Xiao, D. Lohan, F. Arastu, and K. Haran, "High-frequency electric machines for boundary layer ingestion fan propulsor," *IEEE Transactions on Energy Conversion*, vol. 34, no. 4, pp. 2189–2197, Dec. 2019. [Online]. Available: https://doi.org/10.1109/tec.2019.2942775

[46] V. Fedak, P. Zaskalicky, and Z. Gelvanič, "Analysis of balancing of unbalanced rotors and long shafts using GUI MATLAB," in *MATLAB Applications for the Practical Engineer*. InTech, Sep. 2014. [Online]. Available: https://doi.org/10.5772/58378

[47] M. Leader, "A practical guide to rotor dynamics," Applied Machinery Dynamics Company, Tech. Rep., 2004. [Online]. Available: https://rotorbearingdynamics.com/wp-content/uploads/2018/04/A-Practical-Guide-to-Rotor-Dynamics.pdf

[48] B. Alderks, "Slot fill and design for manufacturability," Windings, Inc., Tech. Rep., 2019. [Online]. Available: https://www.windings.com/wp-content/uploads/whitepaper-slot-fill-windings.pdf

[49] M. Lokhandwalla, K. S. Haran, and J. P. Alexander, "Scaling studies of high speed high temperature superconducting generator," in *2012 XXth International Conference on Electrical Machines*. IEEE, Sep. 2012. [Online]. Available: https://doi.org/10.1109/icelmach.2012.6349958

[50] K. Yamaguchi, "Design and evaluation of SiC-based high power density inverter, 70kW/liter, 50kW/kg," in *2016 IEEE Applied Power Electronics Conference and Exposition (APEC)*. IEEE, Mar. 2016.

[51] C. Zhang, S. Srdic, S. Lukic, Y. Kang, E. Choi, and E. Tafti, "A SiC-based 100 kW high-power-density (34 kW/l) electric vehicle traction inverter," in *2018 IEEE Energy Conversion Congress and Exposition (ECCE)*. IEEE, Sep. 2018. [Online]. Available: https://doi.org/10.1109/ecce.2018.8558373

[52] "Electrical and electronics technical team roadmap," US Department of Energy Office of Energy Efficiency & Renewable Energy, Tech. Rep., Oct. 2017.

[53] S. Rogers and S. Boyd, "Overview of the DOE advanced power electronics and electric motor R&D program," in *DOE Vehicle Technologies Office Annual Merit Review and Peer Evaluation Meeting*, June 2014.

[54] H. Ohashi, "Power electronics innovation with next generation advanced power devices," in *The 25th International Telecommunications Energy Conference (INTELEC) 2003*. IEEE, Oct. 2003.

[55] M. Crittenden, "With ultralight lithium-sulfur batteries, electric airplanes could finally take off," *IEEE Spectrum*, Aug. 2020.

[56] S. J. Gerssen-Gondelach and A. P. Faaij, "Performance of batteries for electric vehicles on short and longer term," *Journal of Power Sources*, vol. 212, pp. 111–129, Aug. 2012. [Online]. Available: https://doi.org/10.1016/j.jpowsour.2012.03.085

[57] M. Hepperle, "Electric flight - potential and limitations," in *AVT-209: Workshop on Energy Efficient Technologies and Concepts Operation*. North Atlantic Treaty Organization Science and Technology Organization, Oct. 2012.

[58] H. Löbberding, S. Wessel, C. Offermanns, M. Kehrer, J. Rother, H. Heimes, and A. Kampker, "From cell to battery system in BEVs: Analysis of system packing efficiency and cell types," *World Electric Vehicle Journal*, vol. 11, no. 4, p. 77, Dec. 2020. [Online]. Available: https://doi.org/10.3390/wevj11040077

[59] P. Stenzel, M. Baumann, J. Fleer, B. Zimmermann, and M. Weil, "Database development and evaluation for techno-economic assessments of electrochemical energy storage systems," in *2014 IEEE International Energy Conference (ENERGYCON)*. IEEE, May 2014. [Online]. Available: https://doi.org/10.1109/energycon.2014.6850596

[60] H. Yang, S. Kannappan, A. S. Pandian, J.-H. Jang, Y. S. Lee, and W. Lu, "Achieving both high power and energy density in electrochemical supercapacitors with nanoporous graphene materials," Nov. 2013, arXiv preprint arXiv:1311.1413.

[61] N. A. Thong, "Application of supercapacitor in electrical energy storage system," M.S. thesis, National University of Singapore, Singapore, 2011.

[62] M. Kazimierczuk and R. Cravens, "Application of super capacitors for voltage regulation in aircraft distributed power systems," in *PESC Record. 27th Annual IEEE Power Electronics Specialists Conference*. IEEE, June 1996. [Online]. Available: https://doi.org/10.1109/pesc.1996.548678

[63] R. Brewer, "Electrical energy storage to meet evolving aircraft needs," *SAE International Journal of Aerospace*, vol. 5, no. 2, pp. 467–480, Oct. 2012. [Online]. Available: https://doi.org/10.4271/2012-01-2199

[64] *Wiring Aerospace Vehicle*, SAE International, Aug. 2019, rev. G.

[65] B. Aigner, M. Nollmann, and E. Stumpf, "Design of a hybrid electric propulsion system within a preliminary aircraft design software environment," *Deutsche Gesellschaft für Luft- und Raumfahrt - Lilienthal-Oberth e.V.*, 2018.

[66] S. Gudmundsson, *General Aviation Aircraft Design: Applied Methods and Procedures*, 1st ed. Butterworth-Heinemann, 2014.

[67] "MQ-9 reaper," U.S. Air Force, Sep. 23, 2015. [Online]. Available: https://www.af.mil/About-Us/Fact-Sheets/Display/Article/104470/mq-9-reaper/

[68] C. R. Martel, "Properties of JP-8 jet fuel," Defense Technical Information Center, AD-A 197 270, WPAFB, OH, 1988. [Online]. Available: https://apps.dtic.mil/dtic/tr/fulltext/u2/a197270.pdf

[69] H. Qi, Y. Fu, X. Qi, and Y. Lang, "Architecture optimization of more electric aircraft actuation system," *Chinese Journal of Aeronautics*, vol. 24, no. 4, pp. 506–513, Aug. 2011. [Online]. Available: https://doi.org/10.1016/s1000-9361(11)60058-7

[70] M. Sadraey, *Aircraft Performance: An Engineering Approach*, 1st ed. CRC Press, 2017.

[71] Y. Teeuwen, "Propeller design for conceptual turboprop aircraft," M.S. thesis, Delft University of Technology, Delft, Netherlands, 2017.

[72] "Climbing flight performance," AOE 3104 Course Notes, Dept. of Aerosp. and Ocean Eng., Virginia Tech. [Online]. Available: http://www.dept.aoe.vt.edu/ lutze/AOE3104/climb.pdf

[73] T. Balachandran, J. Reband, M. Lewis, and K. S. Haran, "Co-design of integrated propeller and inner rotor PMSM for electric aircraft application," in *International Electric Machines & Drives Conference*. IEEE, May 2021.

[74] P. J. Masson, M. Breschi, P. Tixador, and C. A. Luongo, "Design of HTS axial flux motor for aircraft propulsion," *IEEE Transactions on Applied Superconductivity*, vol. 17, no. 2, pp. 1533–1536, June 2007. [Online]. Available: https://doi.org/10.1109/tasc.2007.898120

[75] D. Moreels and P. Leijnen, "This inside-out motor for EVs is power dense and (finally) practical," *IEEE Spectrum*, Sep. 2019.

[76] T. Balachandran, D. Lee, N. Salk, and K. S. Haran, "A fully superconducting air-core machine for aircraft propulsion," *IOP Conference Series: Materials Science and Engineering*, vol. 756, p. 012030, June 2020. [Online]. Available: https://doi.org/10.1088/1757-899x/756/1/012030

[77] T. A. Lipo, *Introduction to AC Machine Design*, 3rd ed. Wisconsin Power Electronics Research Center, 2015.

[78] W. E. Roding, "Vernier hybrid wind turbine generators," Ph.D. dissertation, Durham University, Durham, UK, 2001.